On the Calibration of Tianwen-1/Mars Energetic Particles Analyzer (MEPA) Data

Longhui Liu, Yiqun Yu, Jinbin Cao

Beihang University

May, 2024

This document explains the data files of Tianwen-1/Mars Energetic Particles Analyzer (MEPA) archived on Github. The files contain calibrated level-2B data originally downloaded from the Lunar and Planetary Data Release System at National Astronomical Observatories of China: https://moon.bao.ac.cn/web/zhmanager/mars1. For detailed description of MEPA, readers can refer to Li et al.(2021).

The originally downloaded level-2B data files contain the following parameters: UTC-time, Heavy-Ion_Events_Count, Heavy-Ion_Fake_Events_Count, Heavy-Ion_Science_Data, e/p/he_Events_Count, e/p/he_Fake_Events_Count, e/p/he_Science_Data, Divide_Ratio, VA_Temperature, CSI2_Temperature, SI2_Temperature, PSDH_Temperature, Total_Trigger_Count, e/p/he_Trigger_Count, Heavy-ion_Trigger_Count, Penetration_Count, Longitude， Latitude, Altitude, Instrument_Observation_Direction_X/Y/Z, Solar_Incident_Angle, Solar_Azimuth_Angle and X/Y/Z-axis_Position_J2000.

The downloaded level-2B data contains numerous diffusion data (Tang et al., 2020) due to instrumental issues. We calibrate the data by applying a theoretical model of particle distribution to remove the diffusion data and employing statistical methods of random sampling and elimination, and further calculate the differential flux of different species. The method of calculating particle differential flux and the calibration processes are explained in Section I and II, respectively.

It should be noted that the calibrated result is roughly consistent with simulation results of Tang et al.(2020), but in practical applications of the proton flux, high-precision differential flux and integral flux may have errors due to statistical methods (such as extremely large or small proton flux at a certain time). Due to such errors, the ion flux needs to be averaged over a certain period of time to obtain a more realistic value (Fu et al., 2022). The differential flux of alpha particles resembles noises, so the alpha particle data should be used with caution. The electron data is not calibrated due to difficulties in discerning diffusion data.

I. Flux calculation

A detector located in an isotropic particle radiation field, whose detected particle *count rate N* is proportional to the particle *flux J*. The proportional coefficient, or called the *geometric factor G,* can be expressed by the following formula:

$$G = \frac{N}{J} \tag{1}$$

We calculate the *sampling ratio, r,* by dividing e/p/he_Events_Count by e/p/he_Trigger_Count , and differentiate the particle types using the particle energy data in e/p/he_Science_Data to obtain the index of different particles. After completing the elimination of diffusion events, we obtain the Proton/He_Index. We further obtain the particle *counts* (obtaining the value of N) using the on-orbit particle identification criteria (as shown in Table 1) and calculate the *differential flux* (the value of J) using geometric factors (the value of *G*, as shown in Table 2) and the center values of each energy channel (the value of E_c). It is calculated as follows:

$$flux=\frac{counts}{r*G*E_c} \tag{2}$$

Table 1: On-orbit particle identification criteria

Particle Type	PID criteria (ΔE, E andΔE1 all in unit of MeV)
Electron	$\Delta E \bullet E \le 20$ && $\Delta E < 1$ && $\Delta E > 0.05$
Proton	$(20 < \Delta E \bullet E \le 150$ || $(\Delta E \bullet E \le 20$ && $\Delta E > 1))$ && $\Delta E_1 < 1$
Helium	$150 < \Delta E \bullet E \le 1200$ || $(\Delta E \bullet E \le 150$ && $\Delta E_1 \ge 1)$
Heavy ion	$\Delta E \bullet E > 1200$

Table 2: Geometric factors of energy channels for electrons, protons, and alpha particles

Energy channel serial number	Electron		Proton		Alpha particle	
	Energy channel division (MeV)	Electron _Geom (cm^2 sr)	Energy channel division (MeV)	Proton _Geom (cm^2 sr)	Energy channel division (MeV)	He _Geom (cm^2 sr)
1	[0.1,0.13)	0.08	[2, 2.6)	0.20	[25, 29.2)	0.21
2	[0.13,0.18)	0.11	[2.6, 3.3)	0.21	[29.2, 34.1)	0.22
3	[0.18, 0.25)	0.16	[3.3, 4.2)	0.20	[34.1, 39.8)	0.21
4	[0.25, 0.33)	0.19	[4.2, 5.3)	0.21	[39.8, 46.5)	0.21
5	[0.33, 0.45)	0.21	[5.3, 6.8)	0.20	[46.5, 54.3)	0.22
6	[0.45, 0.60)	0.23	[6.8, 8.7)	0.21	[54.3, 63.5)	0.24
7	[0.60, 0.81)	0.23	[8.7, 11.1)	0.22	[63.5, 74.1)	0.24
8	[0.81, 1.10)	0.25	[11.1, 14.1)	0.22	[74.1, 86.6)	0.26
9	[1.10, 1.48)	0.27	[14.1, 18.1)	0.24	[86.6, 101.2)	0.29
10	[1.48, 1.99)	0.30	[18.1, 23.1)	0.26	[101.2, 118.1)	0.32
11	[1.99, 2.69)	0.36	[23.1, 29.4)	0.33	[118.1, 138)	0.39
12	[2.69, 3.63)	0.52	[29.4, 37.6)	0.42	[138., 161.2)	0.51
13	[3.63, 4.89)	0.77	[37.6, 48.0)	0.79	[161.2, 188.3)	0.86
14	[4.89, 6.60)	0.96	[48.0, 61.3)	1.23	[188.3, 219.9)	1.16
15	[6.60, 8.90)	1.07	[61.3, 78.3)	1.44	[219.9, 256.8)	1.39
16	[8.90, 12)	1.20	[78.3, 100)	1.58	[256.8, 300)	1.50

II. Calibration process

We calibrate the proton data based on methods and suggestions provided by the payload development team. As mentioned above, diffusion occurs in the raw data and the distribution of these diffusing data is scattered in the ΔE-E plot (as shown in Figure 1). We firstly remove most of the diffusing data that are not within the desired energy band enclosed by two horizontal lines. By assuming that the effective data follows a Gaussian distribution as a function of log(E*ΔE), the remaining data are then fitted with a combined distribution: Gaussian distribution plus background diffusion, as shown in Figure 2. Based on the sampling ratio, the background diffusion at each time are statistically removed, resulting in the effective data only, as shown by the black line in Figure 2. After converting back into the ΔE-E coordinates, the blue band in Figure 3 demonstrates the effective data extracted from the background.

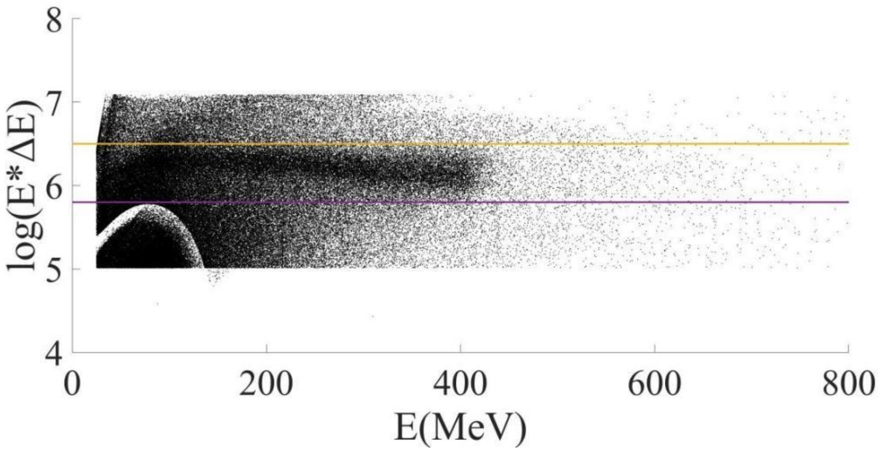

Figure 1: Raw counts data plotted in the log(E*ΔE)-E coordinates. The two curves enclose the energy bands within which the effective data are desired to be extracted.

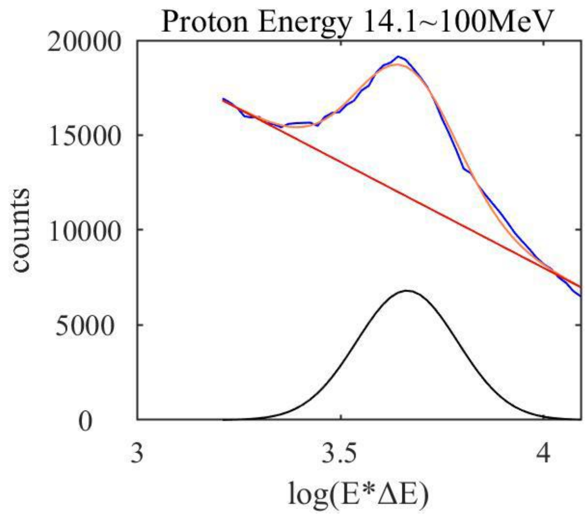

Figure 2: Fitting results of the data with energy from 14.1 to 100MeV. The blue line represents the distribution of data after the operation in Figure 2, the orange curve is the fitted result of data, the red curve is the background diffusion data, and the black curve is the effective data distribution after removing the background diffusion data.

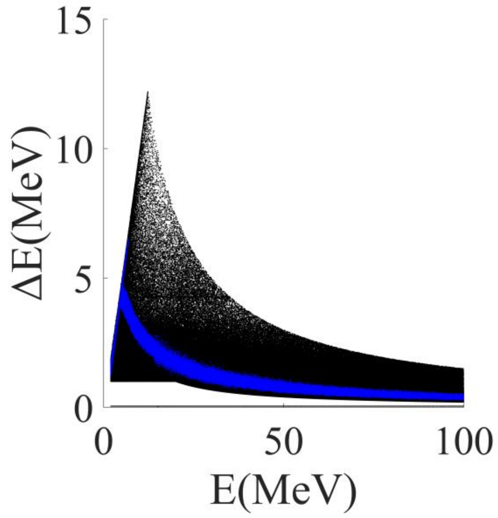

Figure 3: The data in the ΔE-E coordinates, in which the black dots are the background diffusion data and the blue one are the effective data obtained.

The newly calibrated data are all saved in files named as :

HP_xxx_x_xxxxxxxxxxxxxx_xxxxxxxxxx_xxxxx.txt

Here is an example of a filename as follows:

HP_SCI_N_20200724142137_20200724235957_00002.txt

digit 1-2 (HP): the data contains heavy ion data

digit 4-6 (SCI): science data

digit 8 (N): real-time data (data collected directly downstream) and playback data (data stored by the detector and delayed for playback).

digit 10-13: year of the first data sample

digit 14-15: month of the first data sample

digit 16-17: day of the first data sample

digit 18-19: hour of the first data sample

digit 20-21: minute of the first data sample

digit 22-23: second of the first data sample

digit 25-28: year of the last data sample

digit 29-30: month of the last data sample

digit 31-32: day of the last data sample

digit 33-34: hour of the last data sample digit 35-36: minute of the last data sample

digit 37-38: second of the last data sample

digit 40-44: detection cycle number

Table 3: data file structure

Field Name	Field number	Bytes of Each Data	Description
Time	1	14	Coordinated universal time with four-second cadence.
Epoch_Time	2	14	The epoch time format for the IRF package with four-second cadence.
Longitude	3	12	Spacecraft longitude (maybe a nan value).
Latitude	4	12	Spacecraft latitude (maybe a nan value).
Altitude	5	12	Spacecraft altitude (maybe a nan value).
X_J2000	6	17	J2000 Coordinate System.
Y_J2000	7	17	J2000 Coordinate System.
Z_J2000	8	17	J2000 Coordinate System.
X_MSO	9	16	MSO Coordinate System.
Y_MSO	10	16	MSO Coordinate System.
Z_MSO	11	16	MSO Coordinate System.
Instrument_Observation_Direction_X	12	12	Incidence vector of the symmetry axis of the sensor FOV in J2000 Coordinate System.
Instrument_Observation_Direction_Y	13	12	Incidence vector of the symmetry axis of the sensor FOV in J2000 Coordinate System.
Instrument_Observation_Direction_Z	14	12	Incidence vector of the symmetry axis of the sensor FOV in J2000 Coordinate System.
Solar_Incident_Angle	15	6	Solar incident angle.
Solar_Azimuth_Angle	16	6	Solar azimuth angle.
Energy_CSI_1～Energy_CSI_22	17~38	7	The particle energy value detected by the CsI detector (third detector) that is separately distinguished from the original data. Due to the fact that each data packet records 22 events when the detector records particle events, the data is divided into 22 variables for recording, with an energy value format of m * 22 and "m" representing the number of time counts (the same applies to other data recorded as 22 variables thereafter).
Energy_SD1_1～	39～60	7	The particle energy value detected by the

Energy_SD1_22			SD1 detector (first detector) that is separately distinguished from the original data.
Energy_SD2_1～Energy_SD2_22	61～82	7	The particle energy value detected by the SD2 detector (second detector) that is separately distinguished from the original data.
Energy_Total_1～Energy_Total_22	83～104	7	The sum of event energies detected by three detectors.
He_Index_1～He_Index_22	105～126	1	The alpha particle index is obtained by distinguishing particle types based on the energy relationship detected by each detector. A value of 1 corresponds to the energy value of the alpha particle, and a value of 0 represents other particles**.**
Electron_Index_1～Electron_Index_22	127～148	1	The electron index obtained by distinguishing particle types based on the energy relationship detected by each detector, where a value of 1 corresponds to the energy value of the electron, and a value of 0 represents other particles .
Proton_Index_1～Proton_Index_22	149～170	1	The proton index obtained by distinguishing particle types based on the energy relationship detected by each detector, with a value of 1 corresponding to the energy value of the proton, and a value of 0 indicating other particles**.**
He_Sample_Counts_1~He_Sample_Counts_22	171～192	2	The value of alpha particle count.
Electron_Sample_Counts_1～Electron_Sample_Counts_22	193～214	2	The value of electron count.
Proton_Sample_Counts_1～Proton_Sample_Counts_22	215～236	2	The value of proton count.
He_Flux_1～He_Flux_22	237～258	16	Calculated alpha particle flux**.** But the reliability of the results needs to be verified.
Electron_Flux_1～Electron_Flux_22	259～280	16	Calculated electron flux.
Proton_Flux_1～Proton_Flux_22	281～302	16	Calculated proton flux. Take the average of these 22 data points at each time for use.

References

[1] Fu, S., Ding, Z., Zhang, Y., Zhang, X., Li, C., Li, G., Tang, S., Zhang, H., Xu, Y., Wang, Y., Guo, J., Zhao, L., Wang, Y., Hu, X., Luo, P., Sun, Z., Yu, Y., & Xie, L. (2022). First Report of a Solar Energetic Particle Event Observed by China's Tianwen-1 Mission in Transit to Mars. Astrophysical Journal Letters, 934(1), L15. https://doi.org/10.3847/2041-8213/ac80f5.

[2] Li, C., Tang, S., Hu, X., Qian, Y., Wang, Y., Zhao, H., Fu, Q., Sun, Z., He, H., Yu, Y., Zhang, H., Fang, F., Yu, H., Yang, H., Zhao, Z., Zhang, Y., Lin, J., Sun, Z., Tao, W., … Ma, Y. (2021). Design and Realization of China Tianwen-1 Energetic Particle Analyzer. Space Science Reviews, 217(2). https://doi.org/10.1007/s11214-021-00803-0

[3] Tang, S., Institute of Modern Physics, C. A. of S., Wang, Y., Zhao, H., Fang, F., Qian, Y., Zhang, Y., Yang, H., Li, C., Fu, Q., Kong, J., Hu, X., Su, H., Sun, Z., Yu, Y., Zhang, B., Sun, Y., Sun, Z., Science and Technology on Vacuum Technology and Physics Laboratory, L. I. of P., ⋯ National Space Science Center, C. A. of S. (2020). Calibration of Mars Energetic Particle Analyzer (MEPA). Earth and Planetary Physics, 4(4), 1–9. https://doi.org/10.26464/epp2020055

Acknowledgments

This work is supported by the introduction to data processing methods provided by Science and Technology on Vacuum Technology and Physics Laboratory, Lanzhou Institute of Physics. The authors thank the guidance in during the data calibration process from Professor Cunhui Li.